

Approaching a homogeneous galaxy distribution: results from the Stromlo-APM redshift survey

Steve Hatton^{*}

*Department of Physics, University of Durham, Science Laboratories, South Rd, Durham DH1 3LE.
Present address: Institut d’Astrophysique de Paris, 98bis Boulevard Arago, 75014 Paris, France.*

27 April 2017

ABSTRACT

Recent results from a number of redshift surveys suggest that the Universe is well described by an inhomogeneous, fractal distribution on the largest scales probed. This distribution has been found to have fractal dimension, D , approximately equal to 2.1, in contrast to a homogeneous distribution in which the dimension should approach the value 3 as the scale is increased. In this paper we demonstrate that estimates of D , based on the conditional density of galaxies, are prone to bias from several sources. These biases generally result in a smaller measured fractal dimension than the true dimension of the sample. We illustrate this behaviour in application to the Stromlo-APM redshift survey, showing that this dataset in fact provides evidence for fractal dimension increasing with survey depth. On the largest scale probed, $r \approx 60h^{-1}$ Mpc, we find evidence for a distribution with dimension $D = 2.76 \pm 0.10$. A comparison between this sample and mock Stromlo-APM catalogues taken from N -body simulations (which assume a CDM cosmology) reveals a striking similarity in the behaviour of the fractal dimension. Thus we find no evidence for inhomogeneity in excess of that expected from conventional cosmological theory. We consider biases affecting future large surveys and demonstrate, using mock SDSS catalogues, that this survey will be able to measure the fractal dimension on scales at which we expect to see full turn-over to homogeneity, in an accurate and unbiased way.

Key words: cosmology: theory – large-scale structure of Universe – galaxies: clustering.

1 INTRODUCTION

The completion of several large redshift surveys has provided us with the ability to test one of the keystones of modern cosmological thought, the expected homogeneity of the Universe on large scales. Recent debate on this subject (Guzzo 1997) has centred around reports of a fractal distribution of galaxies, such that the measured density of the Universe does not tend to a well defined average as the volume measured increases. Some results appear to support this hypothesis (Coleman, Pietronero, & Sanders 1988; Di Nella et al. 1996; Sylos Labini & Montuori 1998, hereafter SLM); others do not (Scaramella et al. 1998).

In a fractal Universe, the density measured by any observer decreases with the size of the sample considered. This trend produces a bias in conventional, correlation function analysis of galaxy clustering, and is the motivation for employing the statistic known as the conditional density. This quantity is defined in section 2, and its relationship to the

correlation function is explained. In section 3, we show that there exist a number of effects which can bias this statistic. Systematic effects can create the illusion of a density which decreases with scale, even when the underlying distribution is homogeneous. We examine the Stromlo-APM redshift survey (Loveday et al. 1992b; Loveday et al. 1996) in the light of these biases in section 4. Previous work (SLM) has found that the fractal distribution in this catalogue is a constant function of scale, with no turnover to homogeneity suggested. We show that a careful treatment of the biases enables us to reliably probe slightly deeper scales than those of SLM, and that the fractal dimension clearly increases with scale. A comparison is made between the fractal dimension measured from this dataset, and that obtained by analysis of mock Stromlo-APM catalogues taken from N -body simulations. These simulations incorporate a more “traditional” view of galaxy clustering, one in which the amplitude of large-scale anisotropy is given by a CDM model for the galaxy power spectrum. In section 5 we consider the application of the same techniques to larger surveys, in particular

^{*} hatton@iap.fr

the PSCz (Saunders et al. 1994) and the Sloan Digital Sky Survey (Gunn & Weinberg 1995). We conclude in section 6.

2 FRACTAL CORRELATIONS

If clustering in the Universe is described by a fractal, it is not valid to use the conventional definition of the correlation function,

$$\xi(r) = \frac{\langle n(\mathbf{r})n(\mathbf{r} + \mathbf{x}) \rangle}{\langle n \rangle^2} - 1, \quad (2.1)$$

to examine this clustering on scales where the correlation function is small. This is because, on these scales, the shape of this function is affected by the value of $\langle n \rangle$, which has to be estimated from the sample. For a fractal distribution, the measured density will be a decreasing function of the distance from the observer, so there is no well defined $\langle n \rangle$, and the shape of the correlation function will depend on the size of the sample.

The conditional density, $\Gamma(r)$, is defined by

$$\Gamma(r) = \frac{\langle n(\mathbf{r})n(\mathbf{r} + \mathbf{x}) \rangle}{\langle n \rangle} \quad (2.2)$$

(Coleman & Pietronero 1992). Whilst the normalization of this function depends on the mean density of galaxies in the sample, its shape does not. The correlation function is simply related to $\Gamma(r)$:

$$\xi(r) = \frac{\Gamma(r)}{\langle n \rangle} - 1. \quad (2.3)$$

It is clear that in the regime of strong clustering, ie. $\xi(r) \gg 1$, we expect to see $\Gamma(r) \approx \langle n \rangle \xi(r)$.

A fractal distribution with dimension D has the property that the spherically averaged density around an observer obeys the scaling law:

$$N(r) \propto r^D. \quad (2.4)$$

So the conditional density is given by

$$\Gamma(r) = Ar^{D-3} \quad (2.5)$$

where A is a constant for a particular distribution. On small scales, then, we expect to see clustering with a fractal dimension $D = 3 - \gamma$, where γ is the power law slope of the correlation function, generally found to be 1.8 (Davis & Peebles 1983). This $D = 1.2$ dimensionality is indeed observed on the smallest scales ($r \leq 3.5h^{-1}$ Mpc), with a turnover to a fractal dimension of ≈ 2.2 observed for intermediate scales (Guzzo et al. 1991). It should be noted that this steep correlation function on small scales is only observed when the real-space correlation function is measured, either from the angular correlation function or by correcting redshift-space data in some way. The redshift-space correlation function is suppressed on small scales by non-linear peculiar velocities. The magnitude of this effect increases as we look at smaller separations, and so the resulting power-law slope is less steep than that in real space. For example, Fisher et al. (1994) find a power-law slope of $\gamma = 1.66$ in real space, as opposed to $\gamma = 1.28$ in redshift space.

$\Gamma(r)$ is the density in concentric shells of radius r around a point. In order to compare regions of space at different distances from the observer, it is necessary to take a constant

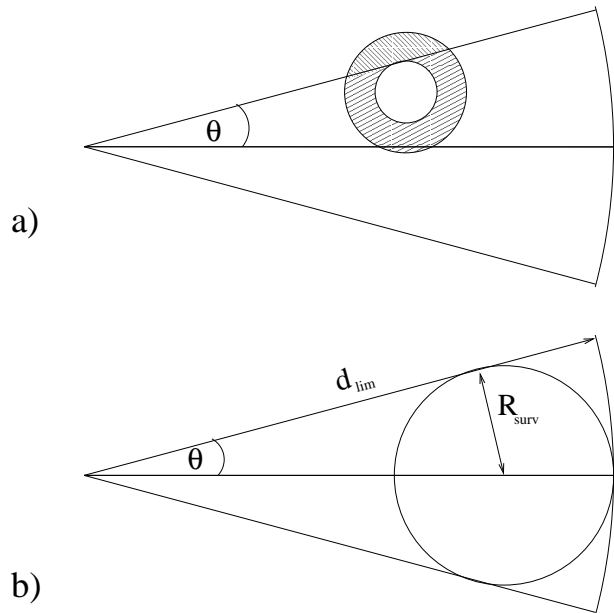


Figure 1. Schematic of a survey wedge. The upper panel illustrates the state of concentric shells around a galaxy in the survey. As the radius of the shell increases, eventually density is measured for shells that are partially external to the survey, such as the shaded shell above. The lower panel demonstrates the maximum distance to which a given survey can probe, the radius of the largest sphere which can totally be contained within the survey.

density, volume limited sample from a redshift survey. This involves discarding a large fraction of the observed galaxies, thus resulting in a rather noisy statistic. For this reason, we will work with the integrated conditional density:

$$\Gamma^*(r) = \frac{3}{4\pi r^3} \int_0^r 4\pi x^2 \Gamma(x) dx. \quad (2.6)$$

This function effectively represents the average density in concentric spheres around the observer. This integration removes noise from the estimate, at the expense of introducing a smoothing and effectively masking any change in the shape of the underlying function. However, over a range of scales for which the distribution is well-described by a single fractal dimension, this statistic will tend towards the same power-law slope,

$$\Gamma^*(r) = \frac{3A}{D} r^{D-3} \quad (2.7)$$

2.1 The maximum scale

As we consider spherical shells around a galaxy at increasing radii, it is clear that we will eventually hit the edge of the survey. Further increases in the shell radius will result in measurements of the density for shells that are underpopulated relative to the mean density. This effect is displayed in the upper panel of Fig. 1. For the outer, shaded shell in this diagram, the measured density will be lower than the true density since it probes a region that by definition contains no galaxies. In conventional correlation function analysis, this effect is corrected for by normalizing to the volume of the shell in question that *is* contained within the survey. This is not appropriate for a fractal distribution, since the

assumption is made that the distribution inside the survey region is the same as that outside. This biases the correlation function, and employing it will tend to mask evidence of a fractal signal. The extent of this bias is debatable. Provenzale, Guzzo, & Murante (1994) find that boundary effects alone cannot mask a true fractal distribution to the extent that the correlation function is as stable and homogeneous on large scales as has been observed. However, the correlation function certainly *is* biased by boundary effects, the only question being exactly how much. Given this point, the motivation exists for adopting the most prudent approach, and we follow SLM in using the $\Gamma(r)$ estimator rather than the correlation function.

For a galaxy i we define r_{\max}^i , the distance to the edge of the survey. Only other galaxies with separation from i less than this distance may be used in the pair counts that contribute to the estimate if the conditional density. This requirement limits the range over which a given survey can measure $\Gamma(r)$; the maximum scale is dictated by the galaxy with the largest r_{\max} . This is equivalent to the radius of the largest sphere that can be contained within the survey geometry, and depends on the opening angle of the survey, θ_{surv} , and the volume limit, d :

$$R_{\text{surv}} = \frac{d \sin \theta_{\text{surv}}}{1 + \sin \theta_{\text{surv}}} \quad (2.8)$$

This is illustrated in the lower panel of Fig. 1.

For a good test of homogeneity, a survey must therefore possess a large opening angle and reasonable depth.

3 BIASES

3.1 Small-scale cut-off

The estimator for $\Gamma^*(r)$ is biased on small scales due to the Poisson nature of the galaxy density field. In Fig. 2 we demonstrate this effect. We have constructed Poisson samples of galaxies and measured $\Gamma^*(r)$ down to small scales. The points and errorbars represent averages and standard deviations over fifty independent realizations. We obtain the expected asymptotic behaviour on large scales for a flat, $D = 3$ power law. On smaller scales, however, the deviation from this homogeneous behaviour is marked. Thus, the signature of a homogeneous distribution can be erased if we attempt to fit a power law down to too small a scale, and it will be necessary to apply a cut-off in our fits.

The precise scale at which the departure from fractal behaviour occurs is not trivial to compute, and will decrease as the fractal dimension of the sample decreases, since a lower fractal dimension results in more clustering and closer pairs of galaxies. However, if one is testing the existence of a turn-over to a homogeneity, it seems prudent to use the small-scale cut-off found for a homogeneous distribution, to remove any potential bias. We will discuss the value chosen for this cut-off in section 4.3.

3.2 Non-constant density

To perform the fractal analysis, it is important to construct a sample with constant density. This is achieved by selecting a volume limited subsample of the redshift survey in question. To construct a volume limited sample, we discard galaxies

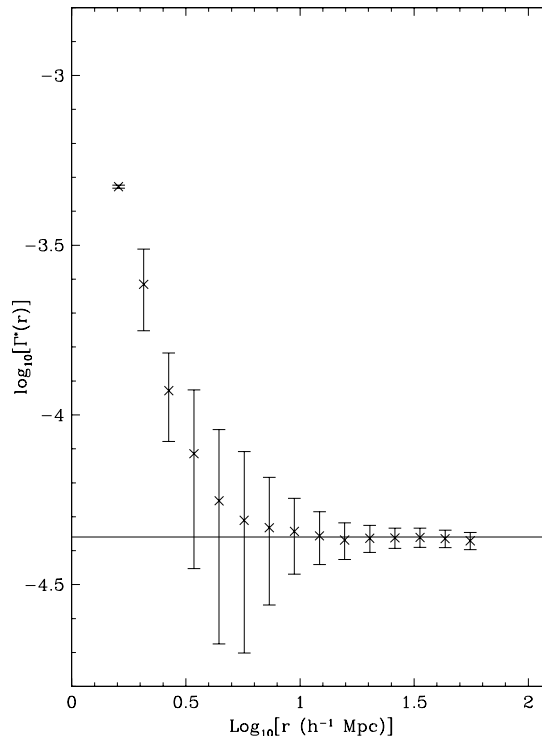


Figure 2. The behaviour of $\Gamma^*(r)$ for a sparse, $D = 3$ (Poisson) sample of points. The horizontal line is the large-scale asymptote.

at redshifts greater than some maximum redshift, z_{lim} . For each galaxy left in the survey, we define a maximum redshift, z_{max} , which is the redshift that a galaxy with that magnitude could be placed at and still make it into the magnitude limit of our catalogue. Galaxies are only kept if their z_{max} value is greater than z_{lim} , ie. they could be seen if they were placed at the limiting redshift of the sample. Several effects can lead to problems with this volume limiting. Failing to correct for them will thus lead to a non-constant density over the sample, which can bias estimates of the fractal dimension. These effects include:

(i) Cosmology. Observations of galaxy positions are made in redshift coordinates, but to measure the clustering in three dimensions we must convert to a Cartesian, comoving coordinate system. This requires knowledge of the function $r(z)$, which depends on the cosmological parameters Ω_0 (mass density) and Λ_0 (cosmological constant). In Fig. 3 we display $r(z)$ for three cosmologies, and compare with the linear relation that is accurate for $z \ll 1$.

The redshift-distance relation also affects the construction of a volume limited subsample of galaxies. We must define a maximum redshift at which each galaxy could be placed and still be within the catalogue magnitude limit. This redshift is calculated via the relation:

$$m - m_{\text{lim}} = 5 \log_{10}[(1+z)r(z)] - 5 \log_{10}[(1+z_{\text{max}})r(z_{\text{max}})] \quad (3.1)$$

It is clear that, in general, if the wrong $r(z)$ is used, we will not produce a constant-density sample of galaxies, and the fractal dimension will be biased.

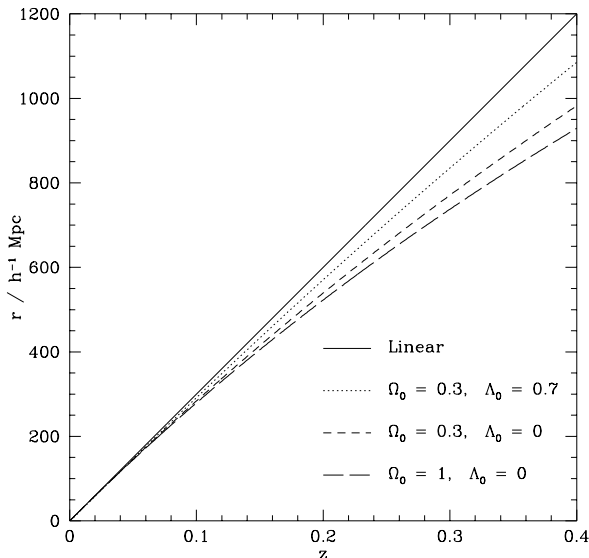


Figure 3. The linear redshift-distance compared with that for three cosmologies, $(\Omega_0, \Lambda_0) = (1, 0), (0.3, 0.7)$ and $(0.3, 0)$

Note that, in a Universe that is truly described by a fractal distribution of matter, the assumption of homogeneity made in deriving the Friedmann equation (Peebles 1993) is no longer valid. Thus, $r(z)$ calculated for any ‘standard’ (Friedmann) cosmology will be inaccurate here, and new formulae for the metric must be derived (although Durrer & Sylos Labini (1998) present an alternative scenario whereby the mass distribution is homogeneous, but the galaxy distribution fractal). Thus, it is possible that an apparent flattening of the conditional density could occur in an inhomogeneous Universe if $r(z)$ from standard cosmology is used. More obviously, it can be seen that employing the wrong cosmological parameters in a homogeneous Universe can lead to a spurious fractal signature.

(ii) Dust. Some galaxies will be thrown out of a volume limited sample if they are in high-extinction areas of sky, since their z_{\max} values appear lower than the volume limit. These galaxies are in fact needed to produce a sample with constant density. It is possible to correct galaxy magnitudes using maps of galactic extinction (Burstein & Heiles 1982; Schlegel, Finkbeiner, & Davis 1998). An additional effect that cannot be corrected for is the suppression of observed galaxy number counts in the high-extinction regions of the sky. Galaxies have been missed by the original survey that are again needed if the volume limited sample is actually to be of constant density. Both these effects will result in a depletion of galaxies at large distances. Thus, even in a homogeneous distribution, the galaxy number density will be seen to fall on the largest scales, a spurious sign of fractal clustering.

(iii) K-correction. As galaxies are redshifted we see a different part of their spectrum. Thus their apparent magnitudes depend on redshift and the shape of this spectrum. The spectral shift generally results in an increase in the apparent magnitude of the galaxy. Thus the inferred luminosities of the galaxies, if we fail to take this k-correction into account, are lower than their true, rest-frame luminosities.

In this case, a volume limited sample will become less dense with distance from the observer, and will tend to underestimate the fractal dimension. Scaramella et al. (1998) have examined the fractal dimension of the ESO slice project, a redshift survey of mean depth $z \approx 0.1$, and find that the choice of k-correction can significantly bias the results for this sample.

(iv) Evolution. Similarly, the intrinsic evolution of a galaxy sample with look-back time results in a different class of objects being selected as the depth of the survey increases. This can again cause variations from uniform density in a volume limited sample. At high enough redshift, the effect of galaxy mergers will ultimately increase the number density on the largest scales.

3.3 Errors in r_{\max}

As explained in section 2.1, for each galaxy we only include neighbours out to the distance to the edge of the survey. If we overestimate the value of r_{\max} for a given galaxy, we will include spherical shells that are partially external to survey. There will be no galaxies in this region, so the shell will appear to be underdense compared to its true density. Thus, again, a homogeneous distribution will be measured to have a fractal dimension $D < 3$. In contrast, if we underestimate r_{\max} , the survey is not used to probe large scales as well as it could be, but no bias is introduced. Errors in r_{\max} , then, tend to result in a lower estimated fractal dimension. This bias will apply on all scales if there are errors on r_{\max} for all the galaxies. It is thus important to measure the distance to the edge of the survey as accurately as possible for each galaxy.

4 APPLICATION TO THE STROMLO-APM CATALOGUE

The Stromlo-APM redshift survey (Loveday et al. 1992b; Loveday et al. 1996) consists of 1787 galaxies in the southern galactic polar region, with magnitude $b_J \leq 17.15$, sampled at a rate of 1 in 20 from the APM Bright Galaxy Catalogue (Loveday 1996) and the APM Galaxy Survey. Clustering in this catalogue has been studied using conventional statistics by Loveday et al. (1992a) and Tadros & Efstathiou (1996), and using the conditional average density by SLM. Here we show how the biases explained in the previous section affect the sample, and how we correct for these biases.

4.1 Determining r_{\max}

As explained in the previous section, it is crucial to accurately measure the distance from each galaxy to the edge of the survey. This is not a trivial task for the Stromlo-APM catalogue, since the survey mask is highly irregular. We derive the angular distance of each galaxy to the survey perimeter by:

- (i) using the APM plate numbers to produce a pixel mask for the survey on a 2048×2048 grid.
- (ii) defining pixels in this mask that are on the angular boundary of the survey.

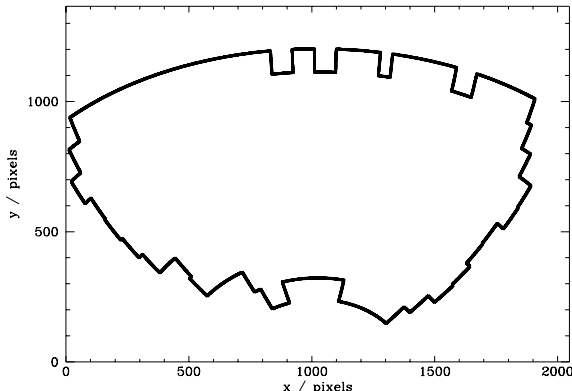


Figure 4. The boundary mask we apply to the Stromlo APM survey to calculate the distance of each galaxy to the edge.

(iii) for each galaxy, finding the boundary pixel with the smallest angular separation, θ_{\min} .

In Fig. 4 we show the mask that results from this treatment. We find for the Stromlo data that this leads to a value $\theta_{\text{surv}} = 22.6^\circ$ for the effective opening angle of the survey. For each galaxy we restrict the pair counts to neighbouring galaxies within $r_{\max} = r \sin \theta_{\min}$, or $r_{\max} = d_{\text{lim}} - r$, whichever is the lesser. We only perform the final fit to the fractal dimension for points that are within the maximum value of r_{\max} for each sample,

The true survey mask in fact contains many small holes due to the presence of bright stars in the field. Since galaxies may in fact be hidden in these holes, a conservative estimate of the distance to the edge of the survey may be given by the distance to the nearest hole. This definition would unfortunately render the survey statistically useless, since it would be unable to probe cosmologically interesting scales. We suggest two possible ways of dealing with this problem, and both will result in a small bias. Firstly, the holes could be filled with a Poisson distribution of particles, having the same selection function as the galaxy sample. These galaxies would be homogeneously distributed, with a well defined average density, and so observations would be biased towards finding a higher fractal dimension. Alternatively, the holes can simply be ignored. This will bias results the other way, since it effectively decreases the homogeneity of the distribution. We choose to adopt the latter scheme.

The accurate values we find for r_{\max} generally enable us to extend our model fits out to greater distances than those used by SLM, effectively probing the dimensionality of the Stromlo-APM sample at larger scales.

4.2 Volume limit errors

From Fig. 3 it will be noted that the low density cosmologies have redshift-distance relationships falling between the linear relation and that for a flat, $\Omega_0 = 1$ Universe. To estimate the maximum systematic error in the Stromlo-APM catalogue arising from the wrong assumed cosmology, we convert redshifts to distances using first the Euclidean, and then the $\Omega_0 = 1$ relationship, and compare the difference.

We k-correct the Stromlo-APM data by subtracting

z_{lim}	d_{lim} h^{-1} Mpc	N	R_{\min} h^{-1} Mpc	R_{\max} h^{-1} Mpc
0.0367	107.2	320	2.0	21.8
0.059	169.5	486	3.2	33.5
0.083	234.5	402	10.0	46.6
0.097	271.4	256	12.0	54.7

Table 1. The limiting redshift, limiting comoving distance, total number of particles, and minimum and maximum scales probed for each of the four volume limited samples we consider.

$a(T)z$ from the apparent magnitude of each galaxy before calculating the z_{max} value, where $a(T)$ is a simple correction depending on the type, T , of the galaxy. We compare this model for k-correction with the results we get if we do not k-correct at all, to get an idea of the potential systematic bias in the fractal dimension.

The survey is so shallow that neither k-correction nor choice of cosmology have any coherent effect on estimates of the fractal dimension. Although the different choices do result in some scatter about the mean, this is rather small compared to the random errors that will be presented in the next section.

We dust-correct the sample using the extinction maps of Schlegel, Finkbeiner, & Davis (1998). This again has a negligible effect on measurements of the fractal dimension, since the Stromlo-APM survey is in a region of rather low extinction.

We conclude, then, that this galaxy survey is not liable to biases incurred by volume limited samples being of non-constant density.

4.3 The small-scale cut-off

Following section 3.1, for each of the four galaxy samples we analyse, we create many random realizations of Poisson samples with the same number density and volume. These are analysed to find the scale at which $\Gamma^*(r)$ becomes significantly different from a flat, $D = 3$ power law. This is used as the small-scale cut-off when fitting a power-law slope to the data.

SLM use arguments involving the small-scale cut-off of the fractal distribution to reach the conclusion that one should not attempt to fit below $\langle l \rangle$, the mean nearest-neighbour distance of galaxies in the sample. The resulting R_{\min} generally comes out rather similar to ours, as can be seen from a comparison with their table 1.

In Table 1 we present the details of the four volume limited samples analyzed in this paper. In each case, R_{\min} and R_{\max} have been computed as described in this section.

4.4 Results

By carefully restricting our method only to the galaxy pairs where the fractal treatment is expected to be valid, we are able to accurately measure the integrated conditional density, $\Gamma^*(r)$, for the four samples whose properties are described in Table 1. Our results are shown in Fig. 5 and Table 2. The error bars on the data in Fig. 5 come from bootstrap resampling of the galaxy sample, with one hundred bootstraps. Mo, Jing, & Boerner (1992) find that, in

z_{lim}	D	ΔD
0.0367	2.21	0.14
0.059	2.31	0.11
0.083	2.62	0.07
0.097	2.76	0.10

Table 2. The fractal dimension for each of the four samples. The quoted uncertainties are $1\text{-}\sigma$ errors on D .

correlation function analysis, the bootstrap method overestimates the error associated with each point, but that this overestimation is compensated for by the failure of a simple χ^2 fit to take into account the covariance between bins. We are thus justified in performing a χ^2 fit to the data points using these bootstrap errors as the variances, and ignoring the bin-bin interdependence. We fit a model of the form shown in equation 2.7 to the data between R_{min} and R_{max} with A and D as free parameters. The error ΔD quoted in Table 2 is the $\Delta\chi^2 = 1$ confidence limit, representing the marginalized $1\text{-}\sigma$ error on the parameter D .

As the deepest sample is found to be close to Poisson ($D = 2.76$), we expect to see the deviation from power-law behaviour due to small-scale bias to appear at roughly the same scale as was found (section 3.1) for a Poisson distribution with the same volume and density. A break does indeed occur in the behaviour of the conditional density at this point, with a steeper slope on smaller scales. Attempting to fit a single power-law over both these regimes would result in significant bias in the estimated value of the fractal dimension. This is also the case for the second deepest sample, but is less significant for the two shallower samples, in which the fractal dimensions are lower, and hence the scales at which the bias affects the conditional density are significantly smaller than their Poissonian values.

Note that, despite being an integrated quantity, $\Gamma^*(r)$ at times changes quite rapidly with scale: this is especially evident in the deeper samples. The fractional change in volume as one goes from one sphere to the next is given by

$$\frac{\Delta V}{V} \simeq \frac{3r^2 \Delta r}{r^3} \simeq 3\Delta \ln r = 3 \ln 10 \Delta \log r. \quad (4.1)$$

Since $\Delta \log r \approx 0.06$, this implies that $\Delta V \approx 0.4V$, so the volume increases by around 40 per cent in each successive bin of Fig. 5. Effectively, then, $\Gamma^*(r)$ can respond quite quickly to changes in the underlying slope of $\Gamma(r)$.

4.5 Comparison with mock catalogues

In order to compare these results with the expected behaviour of the fractal dimension under the assumption of a conventional, CDM-variant cosmology, we have created mock Stromlo-APM redshift surveys using the approach detailed by Cole et al. (1999, hereafter CHWF) for the construction of mock 2dF and SDSS redshift catalogues. Analysis of these simulations, using exactly the same techniques that were previously applied to the real data, also provides a check of our methods. The details of simulations used and biasing methods employed are explained in CHWF. Briefly:

(i) the mock catalogues are drawn from ten independent τ CDM simulations, with $\Omega_0 = 1$, $\Lambda_0 = 0$.

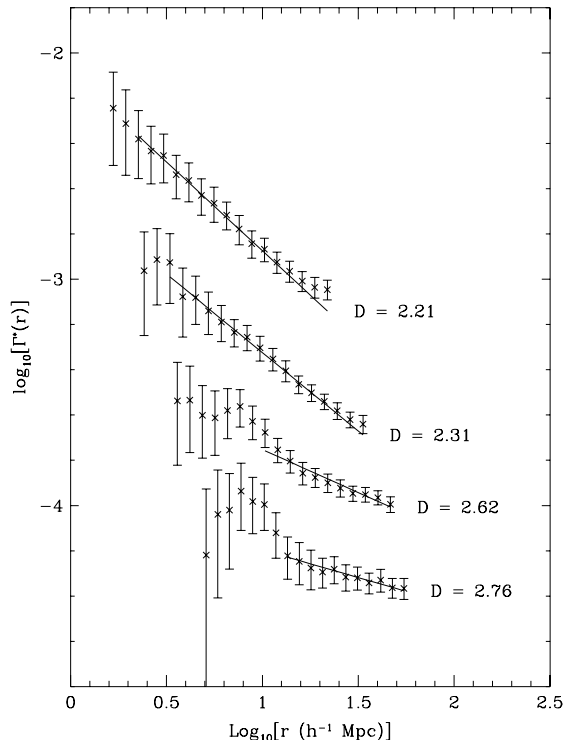


Figure 5. The measured $\Gamma^*(r)$ for the four samples with properties described in Table 1. Error-bars come from one hundred bootstrap resamples. Also plotted are the best fit power-law models, shown only for the range over which they have been fitted.

(ii) the underlying power spectrum is a Bardeen et al. (1986) model with shape parameter $\Gamma = 0.25$, and amplitude $\sigma_8^{\text{mass}} = 0.55$.

(iii) the simulations are biased using CHWF model 1, to obtain a similar level of galaxy clustering to that observed in the APM galaxy survey, ie. $\sigma_8^{\text{gal}} \approx 0.96$ (Maddox, Efstathiou, & Sutherland 1996).

(iv) the selection function used is based on a Schechter (1976) luminosity function with parameters taken from Loveday et al. 1992b ($\alpha = -0.97$, $M^* = -19.5$, $\phi_* = 1.4 \times 10^{-2} h^3 \text{Mpc}^{-3}$).

(v) the catalogues are constructed using the Stromlo-APM mask derived in section 4.1, and thus have the same problems of non-uniform geometry and holes as the true sample.

There is one key difference between our mock catalogues and the real sample, namely that our assignment of luminosities to galaxies pays no attention to the environment of the galaxy. Thus, the clustering for all luminosity classes of galaxies will be the same in our catalogues. This is not necessarily the case for the real sample. Loveday et al. (1995) find that sub- L_* galaxies in the Stromlo-APM cluster more weakly by a factor of two than L_* galaxies, but that galaxies with higher luminosities than this do not show any increase in clustering strength. Since L_* galaxies can be seen up to $\approx 180 h^{-1} \text{Mpc}$, our smallest sample will contain a significant number of fainter galaxies, and therefore may be expected to

z_{lim}	D	ΔD
0.0367	2.41	0.12
0.059	2.40	0.10
0.083	2.64	0.08
0.097	2.73	0.09

Table 3. The fractal dimension measured from mock Stromlo-APM catalogues. The quoted uncertainties the standard deviations of the results about the mean.

appear more homogeneous, relative to the mock catalogues, than the deeper samples. This will not be an important effect for the deeper samples, which only contain galaxies brighter than L_* .

We use the same volume limits as applied to the real Stromlo-APM sample, and present our results in Table 3.

The use of ten mock catalogues enables us to discern firstly whether the bootstrap errors on the fractal dimension are reasonable estimates on the uncertainty of this quantity, and secondly whether the behaviour seen in the Stromlo-APM sample is consistent with the conventional clustering scenario used to construct the mocks. It will be seen from a comparison of Tables 2 and 3 that both these points are satisfied. The bootstrap errors do indeed provide a good estimate on the uncertainty in D , and the value of the fractal dimension as a function of scale shows excellent agreement in the real sample to that taken from the CDM simulations.

We conclude that the use of the fractal dimension as a measure of the homogeneity of the galaxy sample in the Stromlo-APM catalogue in no way discriminates against the conventional picture of clustering. The previously claimed scale-invariant fractal behaviour (SLM, $D = 2.1 \pm 0.1$) is ruled out at the level of several- σ for the deepest galaxy sample.

5 ANALYSIS OF LARGER SAMPLES: SDSS MOCK CATALOGUES

It was shown in the previous section that the Stromlo-APM catalogue is fairly robust to errors in dust correction, k-correction and assumed cosmology, since it is at low redshift and in an area of very low extinction. To illustrate the biases that occur in a deeper sample, will now examine one SDSS mock catalogue, based on the CHWF τ CDM simulation, and four variants:

(i) **MAP.** We add extra long-wavelength power, to this catalogue, via the Mode Adding Procedure (Tormen & Bertschinger 1996; Cole 1997), as described in CHWF.

(ii) **Λ CDM.** The catalogue is drawn from a Λ CDM simulation with $\Omega_0 = 0.3$, $\Lambda_0 = 0.7$. This simulation has the same initial phases as the τ CDM one, and so samples the same structures.

(iii) **Dust.** The galaxies have their magnitudes lowered by the amount corresponding to predictions from the dust maps of Schlegel, Finkbeiner, & Davis (1998). In this case, we boost the selection function used in creating the catalogue such that the number density is the same as for the original catalogue.

(iv) **Evolution.** We use the strong evolution model of CHWF, in which the effects of evolution are not cancelled

Name	D		
	$z_{\text{lim}} = 0.1$	0.2	0.3
Mock	2.78	2.95	2.94
MAP	2.81	2.96	2.97
Λ CDM	2.81	2.94	2.98
Dust	2.82	2.93	2.95
Evol.	2.81	2.98	2.91

Table 4. The observed fractal dimensions from the SDSS mock catalogue and four variants. D is shown for three limiting redshifts, $z = 0.1, 0.2, 0.3$. The typical error on D from bootstrap resampling is ± 0.02 .

out by those of k-correction. Again, the particle number is conserved by changing the amplitude of the selection function.

Apart from the dust catalogue, the construction of these variants is described in detail in CHWF. Since these catalogues all effectively sample the same region of space, any differences between their properties will generally be systematic rather than random. We find that we are able to obtain accurate results out to a redshift limit of $z \approx 0.3$. Fig. 6 illustrates the behaviour of $\Gamma^*(r)$ for the main SDSS mock catalogue. The ability of this sample to probe homogeneous scales is quite evident. Note that we do not apply the same criterion here as used in section 4.3 for determining the small-scale cut-off. The higher sampling rate in the SDSS would result in an attempt to fit a power-law over a wide range of scales, but we do not expect this to be a good fit to the data, since the simulations are constructed with a CDM-like power spectrum which turns over to homogeneity on large scales, and they follow clustering into the non-linear regime on small scales. In this instance, we are not concerned with finding the large-scale behaviour but obtaining an estimate of how well the SDSS will be able to identify homogeneity if it exists, and of the magnitudes of the various biases in the data. Hence, we look for the large-scale, asymptotic behaviour of the distribution, and only fit down to scales where the data are still consistent with this slope. We present results in Table 4 for three volume limited samples, $z_{\text{lim}} = 0.1, 0.2$, and 0.3 .

The first thing to note from this table is the fact that the sample with $z_{\text{lim}} = 0.1$ is consistent with the fractal dimension of the deepest Stromlo-APM samples analysed earlier, as expected since the redshifts are very similar, and the strength of clustering in the two catalogues is the same. Secondly, the samples at $z_{\text{lim}} = 0.2$ are extremely close to the $D = 3$ result expected if homogeneity has been reached.

It should be noted that one of the disadvantages with catalogues drawn from these simulations is that they contain no power on scales larger than the box size, $345.6h^{-1}$ Mpc. Thus, for samples approaching this depth, we expect to see a turnover to homogeneity that may be in excess of that for a CDM model with power on larger scales. We analyse the MAP catalogue, which contains power on much larger wavelengths than this, in order to get an idea of the systematic difference introduced by this extra power. In fact, it will be seen from comparison of the first two rows of Table 4 that the inclusion of this power has negligible effect on the fractal dimension.

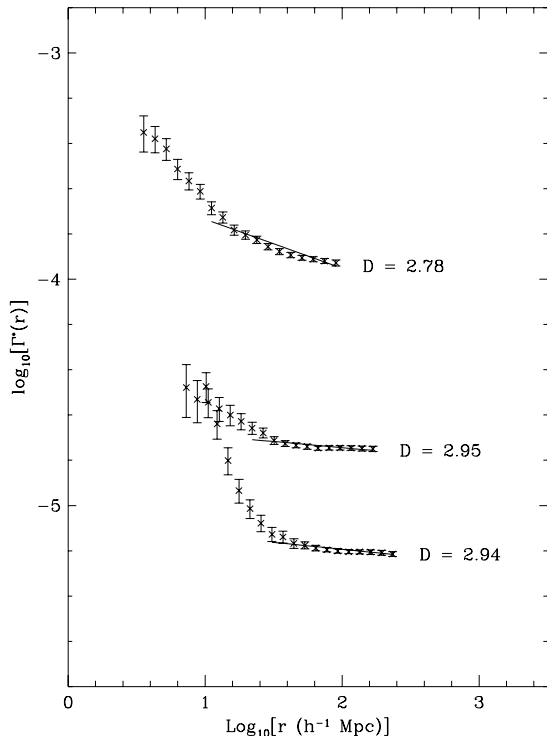


Figure 6. The measured $\Gamma^*(r)$ for the three samples from the straightforward SDSS mock catalogue.

Judging from Fig. 3, we might expect cosmology to be a major factor in biasing deeper the samples from the Λ CDM catalogue since the redshift-distance relations are quite discrepant at these redshifts. This turns out not to be the case. The assumption we have made, of an $\Omega_0 = 1$ cosmology, should result in an artificial squashing of the volume element at high redshift. Thus, the galaxy density would be expected to increase with redshift in a volume limited sample. However, the change in limiting redshift of each particle, described by equation 3.1 has the opposite effect: the value of d_{\max} , the maximum distance (in comoving co-ordinates) at which a particular galaxy can be seen by the magnitude limited survey, is reduced under the $\Omega_0 = 1$ assumption, with the effect of reducing the density at high redshift. The net effect of these two considerations is thus much smaller than either of them taken singly, and the catalogue analysed with the wrong cosmology does not produce significantly different results from the main catalogue. Note that this means we have, on average, intrinsically brighter galaxies at high redshift in the sample. This is not a problem in our mock catalogues, since there is no dependence of clustering properties on galaxy luminosity, but could result in a bias for a real survey.

Similarly, as shown in the final two rows of Table 4, introducing dust and using the wrong model for the effects of k-correction and evolution appear to have little or no appreciable effect on the fractal dimension of the sample at any redshift. This is despite the fact that the SDSS survey extends to quite low galactic latitudes at its southern-most extremities.

We conclude that for the SDSS sample, despite its much greater depth and angular coverage than the Stromlo-APM, there is unlikely to be serious systematic bias caused by any of the volume limit effects outlined in section 3.2.

6 DISCUSSION

We have shown that, contrary to previous results, the distribution of galaxies in the Stromlo-APM redshift survey approaches homogeneity as the sample depth is increased. Galaxies in volume-limited subsamples from the Stromlo-APM catalogue generally cluster as fractal distributions, with higher fractal dimension on for deeper samples.

At the deepest scale that can be reliably probed ($\approx 60h^{-1}$ Mpc), the conditional density of behaves as a power-law, with slope given by a fractal dimension $D = 2.76 \pm 0.10$, close to the value of 3 expected if the Universe is homogeneous. Whilst this is not proof of complete homogeneity on larger scales, we note that:

(i) the value for the fractal dimension is consistent with that expected from a conventional CDM model of galaxy clustering, using parameters for the shape and amplitude of the power spectrum that have been measured from the Stromlo-APM sample itself.

(ii) this value is inconsistent, at the several- σ level, with previous results finding $D = 2.1 \pm 0.1$ (SLM).

We have shown that the fractal dimension measured from the Stromlo-APM survey and indeed future, deeper surveys like the SDSS is generally unaffected by reasonable errors in k-correction, dust correction, and assumed cosmology. Why, then, do our results differ from previously published work? The accuracy of our method for estimating the distance of a galaxy to the edge of the survey, as presented in section 4.1, results in a two-fold gain in probing large-scale inhomogeneities. Firstly, we are confident that there are no errors biasing the fractal dimension on large scales, and, secondly, this confidence enables us to measure the conditional density out to scales around thirty per cent deeper than SLM, where the distribution is closer to homogeneity.

6.1 Application to PSCz

A far more immediate prospect than the SDSS is the application of these techniques to the PSCz survey. This dataset has the advantage that it has a large angular coverage, so, despite having similar depth to the Stromlo-APM, its usefulness in measuring the conditional density at large scales rivals the SDSS. An important factor in extracting the best information from the PSCz will be dealing with its irregular selection geometry. The power of a fully spherically-symmetric survey to probe the largest scales in a statistically valid way is enormous, but the PSCz is restricted by lack of data at low galactic latitudes. Selecting the largest sphere that can be placed in one hemisphere without intersecting with this zone of avoidance reduces the largest scale probed by approximately a factor of two, but the resulting r_{\max} is still large enough that we should expect to see a $D = 3$ dimensionality if the CDM scenario is valid. Further complications arise due to the missing strip of IRAS data that results in a hole in the PSCz data. Since this strip is

basically orthogonal to the zone of avoidance, including it in restricting the size of the sphere results in a severe additional reduction in the maximum scale that can be probed. We suggest that, in order to maximise the useful range of the data, each hemisphere should be analyzed with the strip unfilled, resulting in a bias away from homogeneity, and then padded with a Poisson sample of particles, resulting in a bias towards homogeneity. These extremes should successfully bracket the true behaviour of the sample, resulting in a quantified systematic error on the derived fractal dimension.

ACKNOWLEDGEMENTS

The author acknowledges the support of a PPARC studentship and funding from Durham University. The author would like to thank Shaun Cole and Carlton Baugh for useful suggestions during the final stages of this work. Thanks also to the referee, Luigi Guzzo, for a prompt and detailed report.

REFERENCES

- Bardeen J., Bond J., Kaiser N., Szalay A., 1986, *ApJ*, 304, 15
 Burstein D., Heiles C., 1982, *AJ*, 87, 1165
 Cole S., 1997, *MNRAS*, 286, 38
 Cole S., Hatton S. J., Weinberg D. H., Frenk C. S., 1998, *MNRAS*, 300, 945
 Coleman P. H., Pietronero L., 1992, *Phys. Rep.*, 231, 311
 Coleman P. H., Pietronero L., Sanders R. H., 1988, *A&A*, 200, L32
 Davis M., Peebles P. J. E., 1983, *ApJ*, 267, 465
 Di Nella H., Montuori M., Paturel G., Pietronero L., Sylos Labini F., 1996, *A&A*, 308, L33
 Durrer R., Sylos Labini F., 1998, *A&A*, 339, L85
 Fisher K. B., Davis M., Strauss M. A., Yahil A., Huchra J., 1994, *MNRAS*, 266, 50
 Gunn J. E., Weinberg D. H., 1995, in Maddox S. J., Aragón-Salamanca A., ed, *Wide-Field Spectroscopy and the Distant Universe*, Proceedings of the 35th Herstmonceux workshop. Cambridge University Press, Cambridge, p. 3, astro-ph/9412080
 Guzzo L., 1997, *New Astronomy*, 2, 517
 Guzzo L., Iovino A., Chincarini G., Giovanelli R., Haynes M. P., 1991, *ApJ Lett*, 382, L5
 Loveday J., 1996, *MNRAS*, 278, 1025
 Loveday J., Efstathiou G., Peterson B. A., Maddox S. J., 1992a, *ApJ*, 400, L43
 Loveday J., Maddox S. J., Efstathiou G., Peterson B. A., 1995, *ApJ*, 442, 457
 Loveday J., Peterson B. A., Efstathiou G., Maddox S. J., 1992b, *ApJ*, 390, 338
 Loveday J., Peterson B. A., Maddox S. J., Efstathiou G., 1996, *ApJS*, 107, 201
 Maddox S. J., Efstathiou G., Sutherland W. J., 1996, *MNRAS*, 283, 1227
 Mo H. J., Jing Y. P., Boerner G., 1992, *ApJ*, 392, 452
 Peebles P. J. E., 1993, *Principles of Physical Cosmology*. Princeton University Press, Princeton
 Provenzale A., Guzzo L., Murante G., 1994, *MNRAS*, 266, 555
 Saunders W. et al., 1994, in Proceedings of the 35th Herstmonceux workshop. Cambridge University Press, Cambridge
 Scaramella R. et al., 1998, *A&A*, 334, 404
 Schechter P., 1976, *ApJ*, 203, 297
 Schlegel D. J., Finkbeiner D. P., Davis M., 1998, *ApJ*, 500, 525
 Sylos Labini F., Montuori M., 1998, *A&A*, 331, 809
 Tadros H., Efstathiou G., 1996, *MNRAS*, 282, 1381
 Tormen G., Bertschinger E., 1996, *ApJ*, 472, 14